PAPER • OPEN ACCESS

Role of pre-ionization in NBI plasma start-up of Heliotron J using non-resonant microwave heating

To cite this article: S. Kobayashi *et al* 2021 *Nucl. Fusion* **61** 116009

OPEN ACCESS
IOP Publishing | International Atomic Energy Agency Nuclear Fusion

Nucl. Fusion **61** (2021) 116009 (8pp) https://doi.org/10.1088/1741-4326/ac2105

Role of pre-ionization in NBI plasma start-up of Heliotron J using non-resonant microwave heating

S. Kobayashi[1,*], K. Nagasaki[1], K. Hada[2], T. Stange[3], H. Okada[1], T. Minami[1], S. Kado[1], S. Ohshima[1], K. Tokuhara[2], Y. Nakamura[2], A. Ishizawa[2], Y. Suzuki[4], M. Osakabe[4], T. Murase[4], S. Konoshima[1] and T. Mizuuchi[1]

[1] Institute of Advanced Energy, Kyoto University, Uji, Kyoto 611-0011, Japan
[2] Graduate School of Energy Science, Kyoto University, Uji, Kyoto 611-0011, Japan
[3] Max-Planck Institute for Plasma Physics, 17491 Greifswald, Germany
[4] National Institute for Fusion Science, Toki, Gifu 509-5292, Japan

E-mail: kobayashi@iae.kyoto-u.ac.jp

Received 31 May 2021
Accepted for publication 25 August 2021
Published 23 September 2021

Abstract

Here, we report on role of pre-ionization using non-resonant 2.45 GHz microwave heating ($P_{2.45\,\mathrm{GHz}} < 20$ kW) in plasma start-up of neutral beam injection (NBI) for heliotron configurations in low beam power (P_{NB}) under non-resonant heating condition. A rapid electron heating towards burn-through of the low-Z impurities was observed experimentally in the early phase of beam injection when the seed plasma density produced by the non-resonant heating was enough for the plasma start-up. Beam heating time to the burn-through increased with decreasing the seed plasma density and a critical density condition of the seed plasma for successful start-up was observed experimentally. Proper timing of the gas fuelling is critical for plasma expansion because the beam fuelling is not significant. A 0-dimensional (0D) model analysis of the NBI start-up developed in this study well reproduces the experimental results. The 0D model clarifies the physical mechanism of the NBI start-up using pre-ionization described as follows: (1) the seed plasma produces sufficient beam ions immediately after beam injection, (2) the beam ions heat up electrons that promote the ionization/dissociation of the background neutrals, (3) this process acts as a positive feedback loop resulting in further electron heating towards burn-through. The 0D model analysis shows that the critical density corresponds to the state at which the electron heating by the beam ions is equal to electron power loss due to conduction and ionization/dissociation.

Keywords: NBI plasma start-up, pre-ionization, heliotron configuration

(Some figures may appear in colour only in the online journal)

* Author to whom any correspondence should be addressed.

1. Introduction

Robust and reliable plasma start-up techniques are of importance not only for the tokamak [1–4] but also in Heliotron/Stellarator devices [5–7]. The start-up problem is more prominent in the high-β operation of Heliotron/Stellarator configurations than in low-β operation. The plasma β affects the transport characteristics in advanced Heliotron configurations. The confinement of the trapped particles improves with increasing β as the mod-B contour aligns with the flux surface. In quasi-omigenious configuration, such as those in Heliotron J and W7-X [8, 9], the plasma β influences the degree of symmetry in the poloidal direction in magnetic coordinates. Therefore, operational scenario for high-β plasma formation is required to study the β-effect on the transport characteristics in advanced Heliotron configurations. In such cases, plasma start-up scheme independent of the resonance condition is preferable as the energy confinement and the plasma β have different dependences on the magnetic field strength.

Hence, a start-up technique using high energy neutral beam injection (NBI) has been developed for large helical device (LHD) [10, 11] and advanced stellarator device W7-AS [12]. In LHD, which has major and minor radii (R/a) of 3.7 m/0.64 m, NBI based on the negative hydrogen ion source (beam energy of 100 keV and power of 1.6 MW) was used for plasma start-up [10, 11]. The NBI start-up in W7-AS was demonstrated with a NBI power of 1.6 MW at a magnetic field strength of $B = 2.5$ T [12]. In both the cases, a good confinement for the beam ions was essential to realize NBI start-up. In fact, NBI start-up using deuterium beam was difficult in LHD for $B < 1$ T, because the decrease in the velocity of the deuterium beam ions compared to the velocity of hydrogen ions causes increase in the charge exchange (CX) loss. Therefore, experimental devices with large major radius and high magnetic field strength are preferred for NBI plasma start-up.

To fulfil the condition for NBI start-up, the assist technique for the NBI plasma start-up has been demonstrated in several Heliotron/Stellarator devices. Target plasmas for NBI were initiated using ion cyclotron range of frequencies in compact helical systems [13] or lower hybrid waves excited by a loop antenna in W7-AS [14]. An assessment of NBI plasma start-up in W7-X has been studied using a 0-dimensional (0D) model analysis [15]. Because the W7-X device has short beam path length (0.6 m), pre-ionization was effective to reduce the plasma start-up time by NBI.

In Heliotron J, a medium-sized ($\langle R_0 \rangle / \langle a_p \rangle = 1.2$ m/0.17 m) helical-axis heliotron device with a helical winding coil, we developed a production method for the target plasmas using non-resonant 2.45 GHz microwave [16]. This enabled the NBI plasma start-up even at low NBI power (>0.3 MW), low acceleration voltage (<30 kV) and small device size (∼1 m). Our previous study [17] illustrated the characteristics of seed plasmas produced by the pre-ionization technique. The pre-ionized plasmas with a density in the order of 10^{17}–10^{18} m^{-3} has been produced for a microwave power ($P_{2.45\,\mathrm{GHz}}$) more than 3 kW. This exceeded the O-mode cut-off density of the injected microwave. The energy of the bulk electrons was greater than the ionization potential of carbon ion (CII: 30 eV) but less than the ionization potential of oxygen ion (OIV: 80 eV). The presence of relativistic electrons, which are essential to the mechanism of the pre-ionization, was confirmed experimentally with the synchrotron radiation and hard x-ray emission measurements. The relativistic electrons were produced due to stochastic interactions between the electrons and the microwave-frequency field [18]. While the characteristics of the seed plasmas produced by non-resonant heating was investigated, we did not study the effect of pre-ionization on the NBI plasma start-up assistance of Heliotron J and its physical mechanism.

In this study, the relationship between the seed plasmas and the NBI start-up is investigated. Because the magnetic configuration of Heliotron J is formed before plasma discharge, the plasma start-up until burn-through for the low Z impurity and plasma expansion can be explained independently from the evolution of equilibrium due to the ramp-up of toroidal current commonly observed in the tokamak start-up. We studied the essential physical mechanism of the NBI start-up by focussing on the interactions between the target plasma and NBI.

The organization of this paper is as follows. In the next section, the Heliotron J device and the experimental equipment for the NBI plasma start-up used in our study are explained. The experimental observations of the NBI start-up with regard to the dependence of the electron density of the seed plasmas are described in section 3. In section 4, the calculation results for the 0D model analysis [19, 20], which has been newly developed for the NBI start-up with taking the pre-ionization effect into account, are presented. The analysis reveals the physical mechanism of the plasma formation by NBI to the burn-through with assistance of the pre-ionization.

2. Heliotron J device and experimental apparatus

The plasma volume is 0.68 m^3 in the standard configuration of Heliotron J. Two tangential NBI systems (BL1 and BL2) have a maximum beam power of 0.7 MW each and an acceleration voltage of 30 keV. The path length of each NBI is about 1.6 m. Hydrogen gas is used in the ion source of NBI, while deuterium gas is used for the plasma fuelling. The gas fuelling is controlled using the pre-programmed Piezo-electric valve system. To produce the non-resonant microwave heating, we use a 2.45 GHz magnetron with the maximum power of 20 kW. The microwave with TE10 mode propagates through rectangular waveguides and injects directly from the waveguide into the Heliotron J vacuum chamber. The injected microwave is close to the O-mode oriented in the horizontal direction to the torus centre. A radiometer system in the frequency range of 58–74 GHz is used to measure the radiation intensity from non-thermal electrons. The intensity of the impurity line emission of carbon (CIII: 464.7 nm) and oxygen (OV: 278.1 nm) is measured with two sets of 25 cm monochromator (NIKON: P250) equipped with a photomultiplier tube. An array of absolute extreme ultraviolet (AXUV) photodiode detectors measures the spatiotemporal profile of the photon emission from ultraviolet to x-ray region. The experimental

data is acquired and stored by the data acquisition system of Heliotron J.

3. Experimental observations

3.1. NBI start-up scheme in Heliotron J

The NBI plasma start-up discharge in Heliotron J can be roughly divided into two phases; pre-ionization using non-resonant microwave heating and the main plasma formation by NBI into the pre-ionized plasmas. Figure 1 shows the time evolution of the plasma parameters obtained in a balanced NBI (25 kV, 0.3 MW) discharge assisted by pre-ionization using the 2.45 GHz microwave ($P_{2.45\,\mathrm{GHz}} \sim 7$ kW).

In the pre-ionization phase, as shown in figures 1(*a*)–(*e*), the microwave was launched when the toroidal electric field (E_{Tr}) was almost zero and the neutral gas pressure at the pumping port was approximately 10^{-5} Pa. Neither fundamental nor higher-harmonic electron cyclotron resonance layers existed for the 2.45 GHz microwaves in the confining region because the magnetic field strength was 1.26 T at the plasma axis. During the pre-ionization phase, we observed a high intensity signal of the radiometer ($f \sim 70$ GHz) and the line-averaged electron density $\overline{n}_{\mathrm{e}}$ to the order of 10^{18} m^{-3}. Synchrotron radiation is the main component of the radiation because the optical thickness calculated by the ray tracing analysis for the 70 GHz electromagnetic wave is approximately 3×10^{-3}. The comparison of the frequency spectrum of the radiation with the synchrotron radiation model indicates existence of MeV class electrons accelerated by stochastic acceleration mechanism [17, 18]. For the cases without gas puffing (GP) during the microwave launch, the electron density was in the order of 10^{17} m^{-3}.

Although the effect of the toroidal electric field on the pre-ionization was thought to be limited, initial electrons with sufficient energy were required to start the stochastic acceleration [18]. Some electrons produced during the current ramp-up of the helical coil, which was about 700 ms before the microwave launch, affected the initial condition of the pre-ionization even though the toroidal electric field was approximately equal to zero at the microwave heating turned-on. Toroidal current (I_{P}) of 300 A was observed at the initial phase of the non-resonant microwave launch. The toroidal current decreased with time and became approximately zero before the NBI was turned-on. The formation of the toroidal current by the stochastic acceleration was not so prominent during the experiment.

The time evolution of the carbon (CIII) and the oxygen (OV) line emission intensities suggests that large number of electrons with energies exceeding the CII ionization potential (∼30 eV) were produced during the pre-ionization phase. However, the number of the electrons exceeding the ionization potential of OIV (∼80 eV) was small. The contribution of the impurity line emission due to the collisions with the high energy electrons is considered to be negligible.

The plasma start-up after NBI was further divided into three phases; promotion of ionization by NBI, burn-through for the low Z impurities and plasma expansion phase. As shown in figures 1(*f*)–(*j*), the initial electron density at a balanced NBI (BL1 and BL2) turn-on with total injection power of 0.3 MW was 0.16×10^{19} m^{-3} and continuous gas fuelling was applied before and after the turn-on of NBI. Immediately after the NBI was turned-on, the electron density and the CIII intensity started to increase at $t = 173$ ms. This indicates ionization of the background neutral gas was promoted by the beam injection (promotion of ionization by NBI). This was followed by a small peak of OV intensity at $t = 182$ ms, indicating the plasmas were heated rapidly within 7 ms exceeding the radiation barrier (burn-through) for the low-Z impurities. A significant stored energy (W_{DIA}) appeared 10 ms after the beam injection. These observations illustrated that the role of the pre-ionization in the NBI start-up is to produce the beam ions effectively in the early phase of the NBI injection even in the low NB power condition. This contributes to the electron heating exceeding the radiation barrier. This point will be discussed using the 0D model analysis for the start-up.

The gas fuelling intensified at $t = 193$ ms can increase the electron density more than 1×10^{19} m^{-3}. The radiometer intensity gradually decreased with an increase in the density. Because the microwave power was turned-off at $t = 180$ ms and the electron density increases after NBI, the high energy electrons were thought to be dissipated by the collisions of the background plasmas. Spatiotemporal evolution of the ultraviolet light intensity measured with the AXUV detectors represents characteristics of plasma expansion. The AXUV intensity at $r/a < 0.8$ increased rapidly after the NBI turn-on. This means that the plasma expansion for more than the half radius was achieved within 5 ms after the beam injection. On the contrary, a slow plasma expansion for $r/a > 0.8$ was observed from $t = 180$ ms. The plasma expansion depends on the timing of gas fuelling, which will be described in section 3.3.

3.2. Effect of seed plasma density on burn-through

The seed plasma density at the moment of beam injection affects the burn-through. Figures 2(*a*)–(*c*) show the time evolution of the electron density, OV emission intensity and spatiotemporal profile of the AXUV intensity under the initial density of 0.35, 0.10 and 0.01×10^{19} m^{-3}, respectively. The electron density of seed plasma was controlled by changing the magnetron power and gas fuelling during the microwave launch [17]. The toal NBI power was 0.3 MW, while the magnetron power varied from 5 to 15 kW. The origin of the horizontal axis Δt_{NB} is determined at the moment of the beam injection.

For the higher initial density condition as shown in figure 2(*a*), a peak of the OV intensity just after the beam injection was observed. The gas fuelling during the microwave launch was stopped 7 ms before turning-on NBI. The time delay between the turning-on NBI and the peak of the OV intensity ($\Delta\tau^{\mathrm{OV}}$) was 3.7 ms, which represented that the rapid plasma heating exceeding the radiation barrier was achieved immediately after the beam injection. A significant increase in the electron density up to 0.8×10^{19} m^{-3} was observed, while the density decreased from $\Delta t_{\mathrm{NB}} = 10$ ms because the particle fuelling from NBI was small and could not sustain the plasma density.

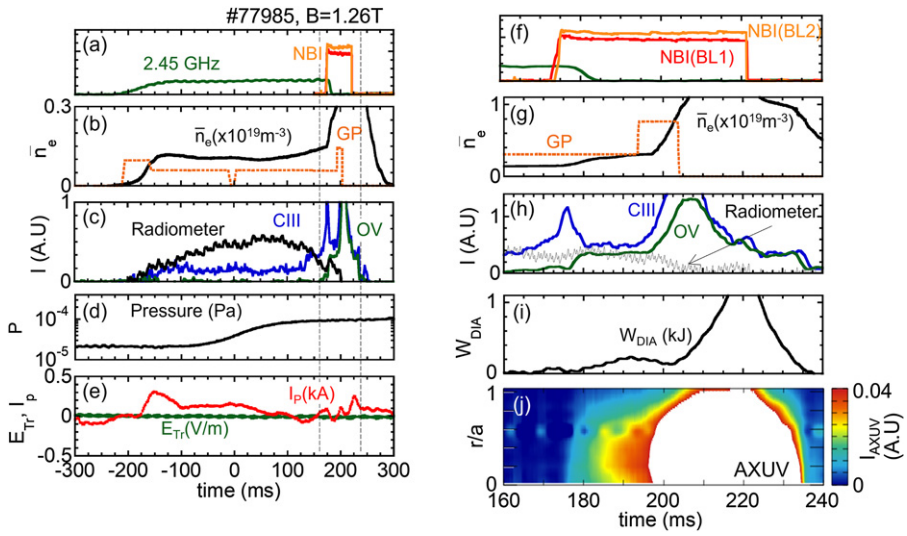

Figure 1. Time evolution of plasma parameters obtained in NBI start-up discharge of Heliotron J assisted by non-resonant microwave heating. (*a*)–(*e*) Pre-ionization by non-resonant microwave launch and (*f*)–(*j*) main plasma formation by NBI. The time response of the neutral gas pressure is in the order of 0.1 s.

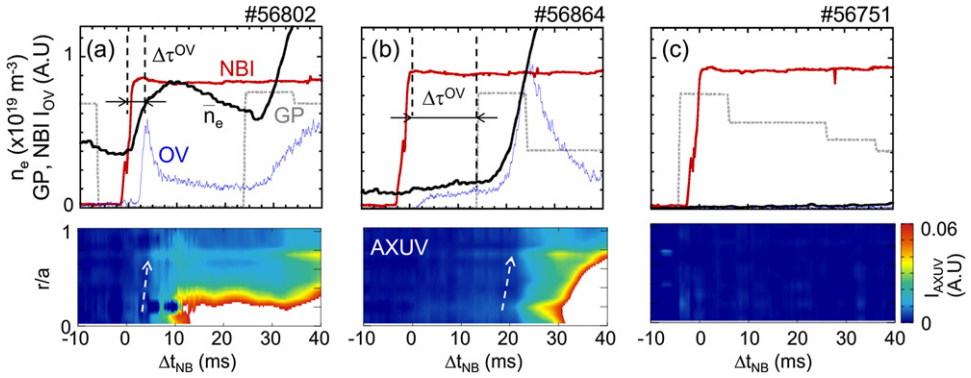

Figure 2. Time evolution of NBI heating, gas fuelling (GP), electron density, OV emission intensity and spatiotemporal profile of AXUV intensity under conditions where initial electron density was (*a*) 0.35 × 10^{19} m^{-3}, (*b*) 0.10 × 10^{19} m^{-3} and (*c*) 0.01 × 10^{19} m^{-3}. The origin of the horizontal axis is determined at the moment of beam injection.

As shown in figure 2(*b*), the increase in the OV intensity delayed and $\Delta\tau^{OV}$ was extended to 13.8 ms for the low initial density condition. The density increase after NBI was not significant as compared with the higher seed plasma density case. The observation suggests that the electron heating by NBI reduces with decreasing the seed plasma density, resulting in the delay of the burn-through. Under a low seed plasma density condition $\bar{n}_e$ of 0.01 × 10^{19} m^{-3} (see figure 2(*c*)), neither density increase nor significant OV intensity were observed. In such the low density case, the NBI start-up was failed under the beam pulse width.

The delay of the peak timing of OV intensity $\Delta\tau^{OV}$ is plotted in figure 3 as a function of the seed plasma density at the moment of NBI turned-on. The microwave power was varied from 5 to 18 kW and the pre-programmed gas fuelling was changed to control the seed plasma density. The NBI power was from 0.3 to 0.4 MW. We obtained a clear relation between the seed plasma density and $\Delta\tau^{OV}$. The burn-through was delayed with decreasing the seed plasma density. Because the burn-through did not occur when the seed plasma density was below than approximately 0.01–0.03 × 10^{19} m^{-3}, the plasma start-up using NBI failed. This means that a critical density condition of the seed plasmas exists for the successful start-up using NBI in Heliotron J. These observations will be compared with the results of the 0D model analysis for the start-up in section 4 to clarify the physical meaning of the critical density.

3.3. Gas fuelling for plasma expansion

The initial density condition and gas fuelling affect the plasma expansion. As shown in figure 2(*a*), the spatiotemporal evolution of the AXUV intensity for the higher initial density case (0.35 × 10^{19} m^{-3}) shows that the plasma expanded rapidly within 10 ms after the peak of the OV intensity. Therefore, NBI power effectively heated the plasmas until the plasma expansion.

For the case of the initial density condition of 0.10 × 10^{19} m^{-3}, as shown in figure 2(*b*), the plasma expansion did not occur until the additional gas fuelling was

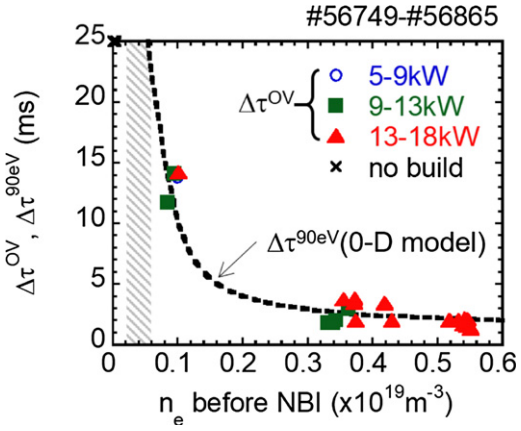

Figure 3. Experimentally observed delay time of OV intensity peak $\Delta\tau^{\mathrm{OV}}$ as a function of seed plasma density at moment of NBI turned-on. Because $\Delta\tau^{\mathrm{OV}}$ for no-build up case cannot be defined, these data are plotted at $\Delta\tau^{\mathrm{OV}} = 25$ ms. Heating time of electron temperature up to 90 eV $\Delta\tau^{90\,\mathrm{eV}}$ calculated in 0D model analysis is plotted as dotted-line.

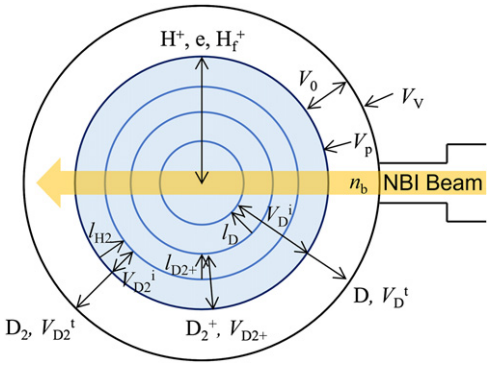

Figure 4. Schematic illustration of 0D model analysis for NBI plasma start-up.

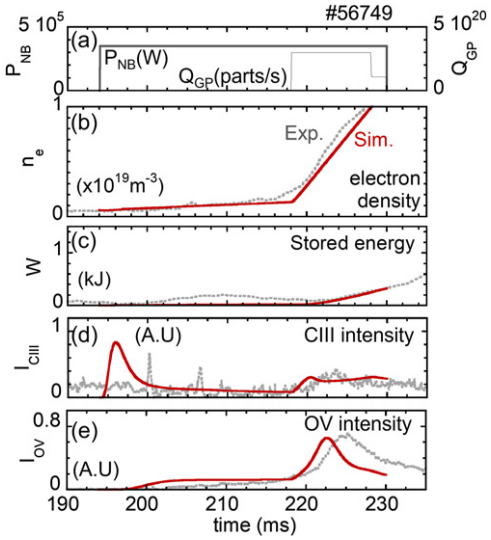

Figure 5. Calculation result of 0D model analysis for NBI plasma start-up and comparison to experimental result. Time evolution of (*a*) heating and fuelling scheme, (*b*) electron density, (*c*) stored energy, (*d*) and (*e*) CIII and OV intensities.

applied at $\Delta t_{\mathrm{NB}} = 14$ ms. The beam absorption calculation for NBI in the Heliotron J shows that the absorbed power fraction is less than 10% when the electron density is less than 0.5×10^{19} m^{-3}. Although a sufficient heating power is required for a plasma expansion, the particle fuelling from neutral beam is not significant to increase the density and beam absorption. An additional fuelling during beam injection is effective to occur the plasma expansion.

In the plasma start-up using NBI in LHD, the gas fuelling at the moment of beam turned-on causes unsuccessful start-up due to large energy loss via inelastic collisions [11]. As shown in figure 1, we observed a rapid plasma expansion even though the gas fuelling was continuously applied under a significant seed plasma density condition. This means that the existence of the seed plasma having significant density can mitigate the requirements for the neutral gas condition. For the case at which the initial density was close to the critical one, on the contrary, the early gas fuelling deteriorates the plasma start-up using NBI. In such the case, the additional fuelling at an appropriate stage such as after the burn-through is essential for achieving the plasma expansion.

4. 0D model analysis

4.1. 0D model for NBI start-up

We developed a numerical analysis code for 0D model of the NBI start-up to clarify the essential process in the plasma start-up by NBI taking the pre-ionization effect into account [19]. Detailed description for the analytical code will be presented in the different paper [20]. The schematic of the code is shown in figure 4. The 0D model enables simultaneous solution of the time dependent particle and energy balance equations. The former represent the fast hydrogen ions (H_f^+) produced by the ionization process of the neutral beam atoms (H_b), the deuterium molecules (D_2) from the gas fuelling, the deuterium molecular ions (D_2^+), the deuterium atoms (D) and the bulk deuterium ions (D^+). Moreover, the energy balance equations represent for the bulk electrons (e) and D^+. The time variation of the fast hydrogen ion density n^+_{fast} is balanced against the sum of the production term of the beam ions by ionization, the CX reactions of the beam atoms, the loss term of beam ions by the CX reactions and the diffusions. In the beam absorption scheme, the beam path length across the plasma volume was 1.6 m. The diffusion term of the beam ion density was set so that the beam ion confinement time would be 0.1 s.

The time variation of the electron internal energy is balanced against the power source from the beam ions by the Coulomb collisions and the cooling due to the electron impact ionization/dissociation, equipartition, conduction and radiation. The heat conduction term was set so that the energy confinement time was 5 ms. The penetration by the neutral hydrogen atoms and molecules is not negligible as compared with the plasma size of Heliotron J (∼0.16 m) under the seed plasma density conditions. Therefore, the penetration length for deuterium atoms, molecules and molecular ions

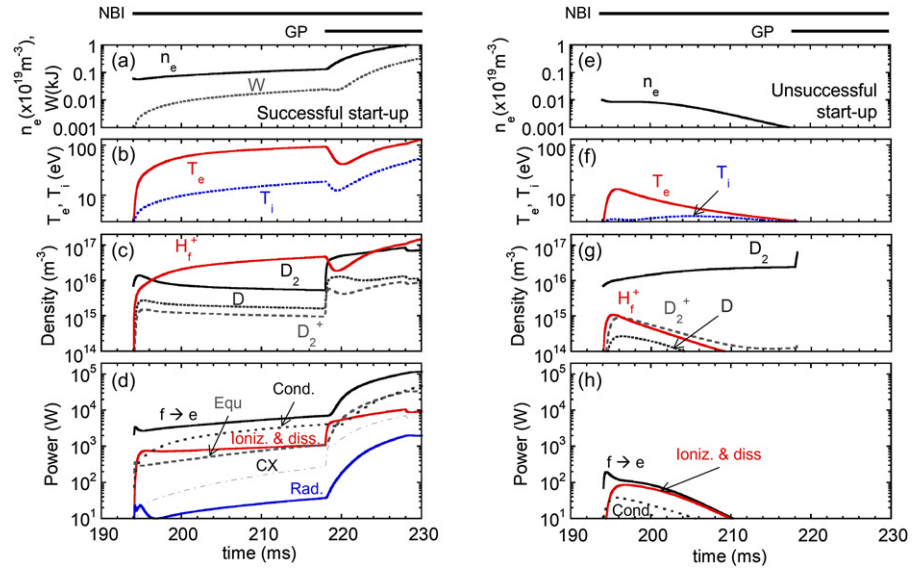

Figure 6. Comparison of densities, temperature and power flow channels calculated by 0D model analysis between (*a*)–(*d*) successful and (*e*)–(*h*) unsuccessful NBI plasma start-up cases.

(l_D, l_{D2}, l_{D2+}) are determined independently by calculating the effective cross sections for these particles. The volume for these particles (V_D, V_{D2}, V_{D2+}) are determined based on the penetration length. Because the ionization/dissociation processes is the main term of the power balance during the initial phase of start-up, the detailed examination of the penetration length of these particles contributes to the precise estimation of the power balance for electrons and fast ions in the 0D model. The volume for the vacuum vessel ($V_V = 2$ m^3) and the plasma ($V_p = 0.68$ m^3) were considered the same as those from the experimental conditions.

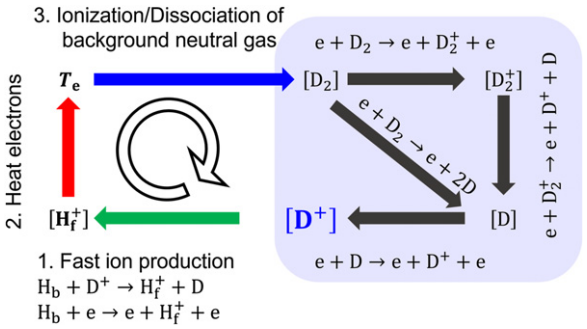

Figure 7. Schematic illustration of dominant mechanism of NBI plasma start-up including seed plasma effects.

4.2. Calculation results

Figure 5 shows the calculation results obtained by the 0D model analysis and comparison with the experimental result. The electron density at the initial condition was set at 0.06×10^{19} m^{-3} and the beam power and the beam energy were 0.35 MW and 25 keV, respectively. We observed a good consistency between the model analysis and the experimental results. A discrepancy was seen in the CIII intensity at the initial phase of the beam injection. In the 0D model, the electron temperature was set to 3 eV and the carbon ion density was zero at the initial condition. Hence, the CIII intensity was overestimated at the initial phase due to the difference in the time evolution of the carbon ion density with the corresponding value from the actual experiment. In fact, we experimentally observed the significant CIII intensity before the beam injection. Because the electron temperature of the seed plasmas has not been obtained due to the detection limit of the YAG Thomson scattering systems in Heliotron J, an improvement of the initial condition of the 0D model analysis is future work after application of electron temperature measurement using impurity line intensity ratio method based on collisional-radiative model [21]. The time evolution of the OV intensity after the beam injection agreed with time evolution from the experiment. After the additional gas puffing $t = 218$ ms, the electron density and stored energy was increased significantly. The calculation was continued until the electron density reached around 1×10^{19} m^{-3}.

Figure 6 shows the comparison of the time evolution of the plasma parameters and the power flow channels between the successful and unsuccessful start-up discharges obtained by the 0D model analysis. The two sets of calculation results differed in only the initial electron density. For the successful start-up case, the initial density was the same as that of the figure shown in figure 5 ($n_e = 0.06 \times 10^{19}$ m^{-3}), and 0.01×10^{19} m^{-3} for the unsuccessful cases. In the successful start-up case, a rapid evolution of the electron temperature was obtained due to the electron heating by fast ions (f → e). The electron heating power increased with increasing the density. The promotion of electron heating led to the dissociation and ionization of the deuterium molecules, molecular ions and atoms. Furthermore, the electron density increase promoted the fast ion production and electron heating. These processes act as a positive feedback loop as shown in figure 7. Hence, the electron temperature increased up to 90 eV within 22 ms after

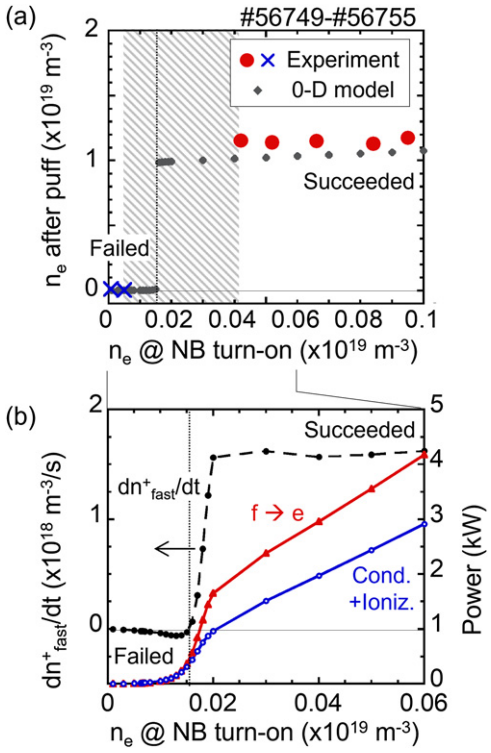

Figure 8. Dependence of electron density at moment of beam injection on (*a*) electron density after additional gas puffing and (*b*) time derivative of fast ion density and heating power dn^{+}_{fast}/dt calculated by 0D model analysis. Hatched region indicates density range that could not be obtained in the experiment.

beam injection leading to successful plasma start-up. Because the electron temperature for the burn-through requires approximately 100 eV [2] and the temperature treated in the 0D model is an averaged value over the plasma volume, the time for electron heating up to 90 eV can be considered as that for burn-through.

The heating power transferred from the fast ions to the electrons is mainly utilized by the conduction term and not by the power losses due to the ionization and equipartition terms. Therefore, the electron temperature is determined by the balance of the fast ion heating and the energy confinement of the electrons. This means that the electron confinement relating to the machine size or magnetic field strength affects the required density of the seed plasmas to succeed the NBI plasma start-up.

For the low initial density condition, the electron temperature did not increase because the production of the fast hydrogen ions remained low. The deuterium molecular density increased with time indicating that the ionization/dissociation of the deuterium molecule was low. In this case, the fast ions lost their energy by the charge exchange reactions to the deuterium molecules. The calculation shows that the electron temperature reached the lower limit (3 eV). Finally, the start-up failed because the positive feedback loop did not occur. Even without gas fuelling and an extended NBI pulse width, the electron temperature did not increase. Therefore the plasma start-up could not be achieved under the condition of the low seed plasma density.

The 0D model can explain the experimentally obtained dependence of the seed plasma density on the start-up. The time required to reach the electron temperature of 90 eV $\Delta\tau^{90\,eV}$ is plotted in figure 3 as a function of the initial density. We obtain a good consistency of the delay time between the observed $\Delta\tau^{OV}$ and the simulated $\Delta\tau^{90\,eV}$. Note that $\Delta\tau^{90\,eV}$ is shortened significantly when the seed plasma density is higher than 0.1×10^{19} m^{-3}. The result supports that the 0D model can simulate the physical processes of the star-up until the burn-through.

5. Discussions

We studied the role of the seed plasmas for the NBI plasma start-up focussing on the experimentally observed critical density condition. Figure 8(*a*) shows the relation between the seed plasma density at the time of the beam injection (corresponding to $t = 194$ ms in figure 6) and the electron density 10 ms after the additional gas fuelling ($t = 228$ ms in figure 6). The experimentally observed critical density condition was reproduced using the 0D model analysis even though the density control of seed plasmas was difficult around the critical density values. The successful plasma start-up was attributed by the occurrence of the positive feedback loop. As described in the previous section, the electrons are heated only by the beam ions. Therefore, the time derivative of the beam ion density dn^{+}_{fast}/dt just after the beam injection is a key parameter to decide the positive feedback loop. As shown in figure 8(*b*), we clearly observe that a positive dn^{+}_{fast}/dt is required for a successful plasma start-up. Above the critical density, the heating power transferred from the fast ions to the electrons begins to overcome the main power loss which is sum of the conduction and the ionization term. The electron heating power increases exponentially around the critical density condition, while the heating power increases linearly with the seed density when the initial density is more than 0.02×10^{19} m^{-3}. These results indicate that the critical density is achieved when the electron heating by the fast ions is balanced against electron power loss by conduction and ionization/dissociation.

6. Summary

We studied the process of NBI start-up assisted by pre-ionization using non-resonant 2.45 GHz microwave heating in Heliotron J. The experimental study and the comparison with the 0D model analysis reveal the role of the seed plasmas in the rapid start-up. The physical processes of the rapid NBI start-up are summarized as follows: (1) the beam ions are produced sufficiently to heat electrons by the collisions with the seed plasmas, (2) the electron heating promotes the dissociation and ionization of the deuterium molecules, molecular ions and atoms, (3) as a result, the increase in the electron density produces the fast ions and further heats the electrons. In the successful start-up cases, the processes act as a positive feedback loop resulting in electron temperature exceeding radiation barrier for the low Z impurities. For the particle fuelling,

beam fuelling does not increase the electron density effectively. Therefore, additional gas fuelling with proper timing is required for plasma expansion at low seed plasma density condition. The key point for the success of the plasma start-up in the low NBI power condition is to produce the beam ions by the collisions with the seed plasmas to heat the background electrons sufficiently in the early phase of the beam injection. The pre-ionization technique developed in our research will be useful for NBI plasma start-up in the low power absorption case such as the perpendicular or deuterium NBI.

Acknowledgments

The authors would like to acknowledge the Heliotron J staff for conducting the experiments. This work was partly supported by the JSPS Grants-in-Aid for Scientific Research Kiban (B) No. 19H01875 and JSPS core-to-core program 'PLADyS', A. Advanced research networks, as well as the collaboration program of the Laboratory for complex energy processes and the Joint Usage/Research Center for Zero Emission Energy Research, IAE, Kyoto Univ. and NIFS Collaborative Research Program (NIFS10KUHL030, NIFS18KUHL087).

ORCID iDs

S. Kobayashi https://orcid.org/0000-0003-1075-2401
K. Nagasaki https://orcid.org/0000-0001-6423-1754
T. Minami https://orcid.org/0000-0003-1125-931X
S. Ohshima https://orcid.org/0000-0003-1341-4969
A. Ishizawa https://orcid.org/0000-0002-5323-8448
Y. Suzuki https://orcid.org/0000-0001-7618-6305
M. Osakabe https://orcid.org/0000-0001-5220-947X

References

[1] Lloyd B. and Edlington T. 1986 *Plasma Phys. Control. Fusion* **28** 909
[2] Jackson G.L., Austin M.E., deGrassie J.S., Hyatt A.W., Lohr J.M., Luce T.C., Prater R. and West W.P. 2010 *Fusion Sci. Technol.* **57** 27
[3] Kajiwara K., Ikeda Y., Seki M., Moriyama S., Oikawa T. and Fujii T. (JT-60 Team) 2005 *Nucl. Fusion* **45** 694
[4] Lloyd B., Carolan P.G. and Warrick C.D. 1996 *Plasma Phys. Control. Fusion* **38** 1627
[5] Nagasaki K. *et al* 2005 *Nucl. Fusion* **45** 13
[6] Cappa Á. *et al* 2015 *Nucl. Fusion* **55** 043018
[7] Wolf R.C. *et al* 2019 *Plasma Phys. Control. Fusion* **61** 014037
[8] Sano F. *et al* 2005 *Nucl. Fusion* **45** 1557
[9] Klinger T. *et al* 2019 *Nucl. Fusion* **59** 112004
[10] Kaneko O. *et al* 1999 *Nucl. Fusion* **39** 1087–91
[11] Kaneko O., Takeiri Y., Tsumori K., Oka Y., Osakabe M. and Ikeda K. (LHD Experimental Group) 2002 *Nucl. Fusion* **42** 441–7
[12] Ott W. and Speth E. (W7-AS Team) 2002 *Nucl. Fusion* **42** 796–804
[13] Kaneko O. *et al* 1990 *Proc. 13th Int. Conf. on Plasma Physics and Controlled Nuclear Fusion Research* vol 2 (Washington DC, Vienna) (IAEA) 473 (http://www-naweb.iaea.org/napc/physics/FEC/STIPUB844_VOL2.pdf)
[14] Ballico M (W7-AS Team) 1993 Stellarator News **29** 4 (https://stelnews.info)
[15] Gradic D., Dinklage A., Brakel R., McNeely P., Osakabe M., Rust N. and Wolf R. (the W7-X Team) (the LHD Experimental Group) 2015 *Nucl. Fusion* **55** 033002
[16] Kobayashi S. *et al* 2011 *Nucl. Fusion* **51** 062002
[17] Kobayashi S. *et al* 2020 *Plasma Phys. Control. Fusion* **62** 065009
[18] Laqua H.P., Chlechowitz E., Otte M. and Stange T. 2014 *Plasma Phys. Control. Fusion* **56** 075022
[19] Hada K. 2015 Model analysis on plasma start-up for toroidal fusion devices *PhD Thesis* Kyoto University
[20] Hada K. *et al* *Plasma Fusion Res.* (private coomunication)
[21] Schweer B., Mank G., Pospieszczyk A., Brosda B. and Pohlmeyer B. 1992 *J. Nucl. Mater.* **196–198** 174